Statistics of passive scalar released from a point source in a turbulent boundary layer

K. M. Talluru[1], J. Philip[2], and K. A. Chauhan[1]

[1]School of Civil Engineering, The University of Sydney, NSW 2006 AUSTRALIA

[2]Department of Mechanical Engineering, The University of Melbourne, VIC 3010 AUSTRALIA

Abstract

In this paper, we report statistics of concentration measurements obtained using photo-ionisation technique. The primary objective of this study is to establish a systematic procedure to acquire accurate single-point concentration measurements in a TBL. Here, we outline procedures implemented in our experiments resulting in concentration profiles that agree very well with previous similar measurements. Passive scalar is released from a point source in the logarithmic region of the boundary layer, and statistics of concentration fluctuations are discussed. Results for mean and variance profiles of scalar fluctuations adhere to the known reflected Gaussian behaviour. Preliminary results for probability density functions of concentration exhibit exponential behaviour with an invariant decay exponent and this is being further investigated.

Introduction

Environmental concerns due to the spread of urban areas is increasingly demanding a better prediction of hazardous gases released from a ground level or an elevated source in the atmospheric boundary layer. The risks associated with dispersion of atmospheric contaminants can be broadly classified into two categories - chronic and accidental. Chronic risks may be estimated using the information of mean concentration field while in the case of accidental risks, one has to properly evaluate potential health hazards from incidental exposure to excessive concentration levels. For this, detailed information of scalar variance and probability distribution functions (PDF) of scalar fluctuations is required. Due to the highly turbulent and intermittent nature of the mixing process, regions of high concentration exist within the plume and often greatly exceed the mean value. It is such extreme events, for example, when the instantaneous concentration level of a gas exceeds its flammability limit, that could lead to spontaneous ignition of a gas and thus initiate a fire.

Although statistics of PDF is most desirable, they are difficult to obtain in practice, as it requires steady flow conditions and long duration samples of concentration fluctuations. In the past, there have been few experimental studies of concentration in laboratory wind tunnels ([1, 8, 9]) and in atmospheric surface layer ([12]) using a point source tracer gas. Most of the above studies were conducted in either atmospheric conditions or artificially stimulated boundary layers and focussed on reporting statistics of scalar fluctuations and their pdfs to develop models for predicting the dispersion of a plume. There are mainly two measurement techniques reported in the literature that can continuously measure concentration fluctuations, namely, flame ionisation detection (FID) and photo-ionisation detection (PID). Both techniques have similar operating principle of ionising a hydrocarbon gas and measuring the voltage output which is a function of the concentration of ions present in the flame/ionisation chamber. In FID, one uses flame to ionise the gas while in PID, it is done using high intensity ultra violet light.

[1] and [9], both using FID technique, have shown that the mean

and variance of scalar fluctuations exhibit either reflected Gaussian or normal Gaussian behaviour depending on the source height. A ground level plume tends to disperse in a Gaussian distribution (to a close approximation) while an elevated plume exhibits reflected Gaussian behaviour. Further, [1] employed the meandering plume model of [2] and the results of [4] to argue that the meandering nature of a plume is the major source of concentration fluctuations. While these results are quite useful in developing prediction models, it is noted that the interaction between the gas plume and the so-called canonical turbulent boundary layer (hereafter, TBL) is rarely investigated. The main motivating factor to this study is the recent developments in the knowledge of the structure of TBL, see for example, [10, 7]. However, most studies on smooth wall TBLs focussed on velocity statistics and were aimed to understand the dynamics between different scales in the flow. The behaviour of concentration fluctuations in a high Reynolds number (*Re*) TBL has not yet been studied. The long term aim of the current study is to relate the characteristics of plume spread to the structure of TBL and as a first step towards that goal, we report here measurements of velocity and concentration fluctuations when a passive scalar is released in the log-region of a TBL.

Experimental setup

The experiments are carried out in the closed-loop Boundary Layer Wind Tunnel (BLWT) in the School of Civil Engineering at the University of Sydney. The working section of the wind tunnel is 19 m long and is 2.5 m wide. It has a constant roof height in the region, $0 \leq x \leq 12$ m, followed by an arrangement of horizontal slats in the roof which can be adjusted to control the pressure gradient between 12 m and 17 m from the trip (a 100 mm wide P60 grit sandpaper spanning the full width of the tunnel). The boundary layer develops on the bottom wall of the tunnel, which is built using plywood sheets and joined together in a seamless manner.

The flow is driven by a 250 kW motor. This flow then passes through a settling chamber comprised of honeycomb flow-straightener and a series of four mesh screens before entering the contraction (with an area ratio of 4.5:1) and then the test section. The free stream velocity can be varied between 0 and 27 m/s. With the wind tunnel in the present configuration, the free-stream turbulence intensity is nominally in the range 0.5% for a free stream velocity range of 0 - 20 m/s. Separate measurements of velocity and concentration are made using a single hotwire and a fast response mini photo-ionisation detector (PID) supplied by Aurora Scientific. A schematic of the experimental setup is shown in figure 1, where different parameters are shown. This experimental set-up allowed us to produce a friction Reynolds number, $Re_\tau = \delta U_\tau / \nu \approx 10{,}600$ (U_τ is the friction velocity and ν is the kinematic viscosity of air). A mild favourable pressure gradient (about 3%) is observed in the current setup. Full details of the boundary layer are listed in table 1. In this paper, x and z refer to the streamwise and wall-normal directions while u denotes the streamwise fluctuating velocity component.
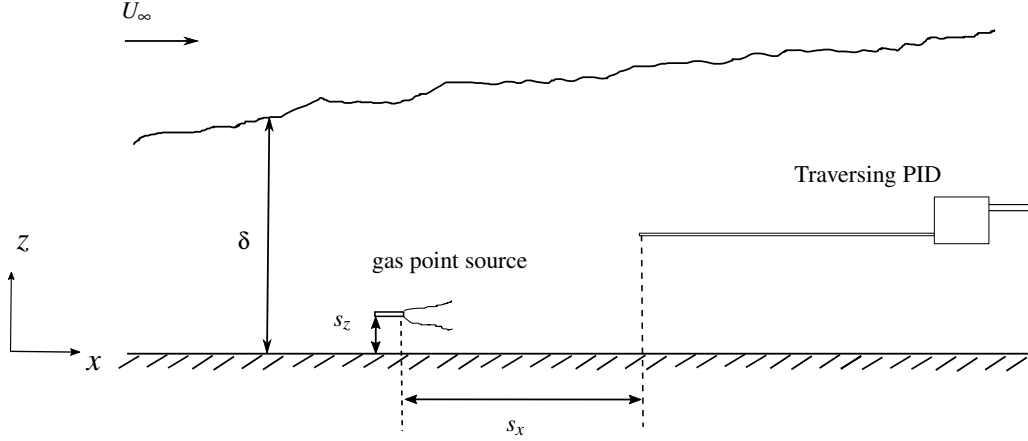
Figure 1: Schematic of experimental setup. s_z and s_x represent the source height and separation distance between source and the measurement location, respectively.

Probe type	Re_τ	Re_θ	U_∞ (ms^{-1})	ν/U_τ (μm)	U_τ (ms^{-1})	δ (m)	θ (m)	$l^+ = \frac{lU_\tau}{\nu}$	$d^+ = \frac{dU_\tau}{\nu}$
Single wire	7 850	14 300	10.2	42.5	0.367	0.329	0.027	24	18

Table 1: Boundary layer properties.

Hot-wire Anemometry

The single-wire probe is a slightly modified Dantec 55P15 type sensor and has a spacing of 1.05 mm with 5 micron diameter Platinum coated Tungsten wire welded between the prongs. The length to diameter ratio of the hotwire is around 210, keeping with the recommendations of [5] and the viscous-scaled wire length, l^+ is about 26. The single-wire is operated using a Dantec multichannel CTA (constant temperature anemometer) at an overheat ratio of 1.8. For the velocity measurements reported, the filter cut-off frequency is set at 10 kHz and the data is sampled at 20 kHz/channel for 300 seconds. Hot-wire is calibrated statically before and after every experiment against a Pitot-static tube located in the undisturbed free stream flow. A total of 10 different flow velocities ranging between 0 ms^{-1} and 12 ms^{-1} are used during the calibration. A third-order polynomial is fitted between the measured hot-wire voltage and the corresponding velocity during the calibration. Besides velocity, temperature is continuously measured in the free stream for the entire duration of the experiment using a fast response copper tip RTD (resistive temperature device) sensor by Omega, Inc. with a response time of 1 sec. It is noticed that the temperature of the flow gradually increased between 1°C and 2°C from the start to the end of a 3 hour long experiment. Hence, a temperature correction scheme (one of the methods discussed in [11]) is employed to correct the drift in hot-wire during the experiment.

Photo-ionisation detector

The PID consists of sensor head, which contains the ultra violet (UV) lamp, electronics, inlet needle (57 mm long and internal diameter (d) of 0.76 mm), a pump, detection cell, and a pre-amplifier. The high energy UV lamp ionizes gases that enter the detection cell. The detection cell and pre-amplifier are built into the end of the sensor head and convert gas concentration to a voltage signal. The use of PID for concentration measurements had been previously established in the study of [8], where flow disturbance due to the sensor head, frequency response and spatial resolution of the sensor were discussed. The inner-normalised diameter (d^+) of the needle is approxi-
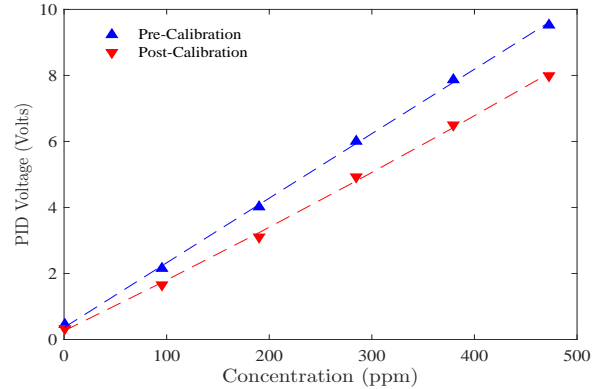

Figure 2: Pre- and post-calibration curves of PID. The dashed lines are second-order polynomial fits using least squares regression.

mately 18. The sensor has a true frequency response of 330 Hz with a 10-90% rise time of 0.6 ms (milli-seconds). The detection limit is 100 ppb (parts per billion) of iso-butylene (or any other ionisable gas) in air and the full-scale measurement range is 500 ppm (parts per million).

The PID is calibrated in situ before and after every experiment using an in-house built manual calibrator. The calibration system consists of a gas-mixing rotameter (manufactured by Matheson Gas Products, Inc.), two mass flow controllers and the necessary tubing and fittings required to connect the outlet of the rotameter to the PID. Both the zero air and 1.5% iso-butylene are available in high pressure cylinders from Airliquide, Inc. They are fitted with two-stage regulators to accurately regulate the outlet to 20 psi gauge pressure as required for the gas-mixing rotameter. It is important to note that this method is a volumetric mixing operation and therefore the pressures and temperatures of the two gases must be the same for better accuracy. A desired concentration of gas is achieved by setting the flow rates of zero air and calibration gas. An example of pre- and post-calibration
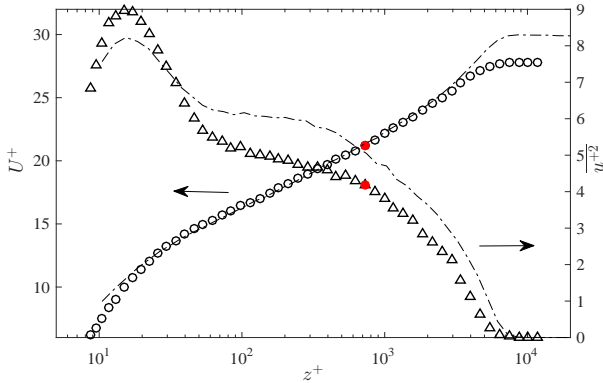
Figure 3: Comparison of mean velocity ($\bigcirc$) and turbulence intensity ($\triangle$) profiles in the current study against comparable zero-pressure gradient boundary layer data ($Re_\tau \approx 8\,400$) of [6]. The red markers show the location of the point source used in this experiment.

curves in one of the experiments is shown in figure 2.

A point source tracer gas (1.5% iso-butylene) is released via a discharge tube of internal diameter 1.6 mm positioned at a height, $s_z/\delta = 0.1$ above the floor (see the schematic in figure 1). The flow rate of tracer gas is adjusted to match the exit velocity to the local mean velocity at the source height in the boundary layer. Since the wind tunnel used in this study is a closed loop type, the background concentration increases with time due to recirculating air in the wind tunnel. It is observed that the background concentration increases linearly with time. Hence, a linear interpolation in time between pre- and post-calibrations of PID is used to correct the drift in PID.

Results

In this section, the mean statistics of the boundary layer are compared against published data. This is followed by a discussion on flow distortion due to PID and finally, the mean, root mean square (r.m.s) and PDF of concentration fluctuations are discussed.

Mean and turbulence intensity profiles

Figure 3 shows the inner-normalised mean velocity and turbulence intensity profiles in the current study in comparison to the comparable Re_τ data of [6] on a smooth wall zero-pressure gradient turbulent boundary layer. It is evident that there are some dissimilarities between the two profiles and these are due to the mild streamwise favourable pressure gradient in our experimental setup. We have verified that this is consistent with the observations of [3], who compared results in a favourable, zero- and adverse pressure gradient boundary layers. They reported that the mean velocity profile in a favourable pressure gradient has a lower wake in comparison to the zero pressure gradient case. Note that friction velocity, U_τ has been obtained by fitting a log-law to the mean velocity profile using constants $\kappa = 0.384$ and $A = 4.17$.

Flow distortion due to PID

Prior to conducting scalar measurements in the turbulent boundary layer, a series of experiments are conducted to understand the influence of discharge tube and PID pump on the flow. Three different scenarios are considered; (i) flow without PID, (ii) flow when PID is activated, and when (iii) deactivated. A single hotwire is used to measure the turbulence statistics in all the three cases. Results reported here have been tested for repeata-
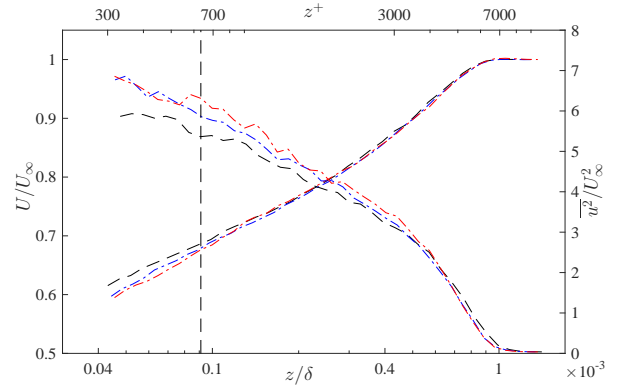

Figure 4: Comparison of mean velocity and turbulence intensity profiles; single wire with no blockage (black dot-dashed lines); single wire when PID pump is activated and deactivated (red and blue dot-dashed lines) respectively. The vertical dashed line represents the physical location of point source.
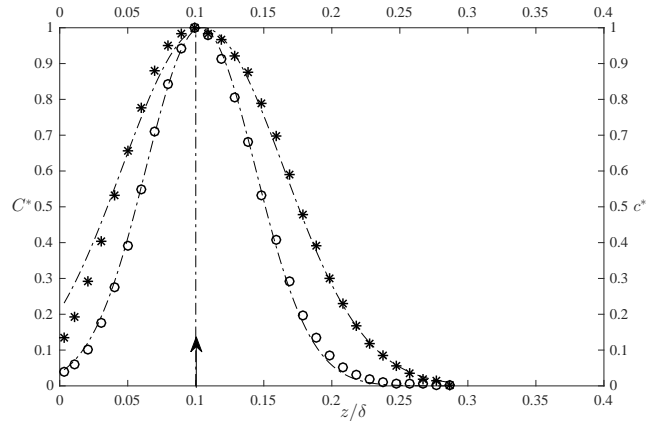

Figure 5: Normalised mean (C^*, $\bigcirc$) and variance (c^*, $*$) profiles of scalar fluctuations as a function of wall-normal distance for $s_z/\delta = 0.1$. The dashed lines are drawn using the reflected Gaussian model (1). The arrow indicates the physical location of the point scalar source.

bility and they are found to be consistent to within $\pm 1\%$. Looking at the mean velocity profiles shown in figure 4 for the three cases, it appears that the discharge tube has caused the flow to decelerate, especially in the near-wall region, $z/\delta \leq 0.08$. The PID operation (pump on and off) seems to have no discernible effect on the mean velocity profile. Looking at the turbulence intensity profiles, there is significant impact; close to the wall, there is an increase of approx. 5% and the effect seems to sustain upto $z/\delta \approx 0.2$. These observations are consistent with [8], who also commented that the near wall discrepancies in the mean flow statistics are due to the proximity of PID to the wall. Overall, we believe that the flow distortion caused by the discharge tube will only influence the scalar statistics as much as it has on the turbulence intensity profile and the results presented below have to be interpreted accordingly. Investigation is currently underway to develop an improved arrangement of discharge tube to release tracer gas with minimal influence on the flow.

Mean and variance profiles of scalar

The normalised mean ($C^* = C/C_m$) and r.m.s ($c^* = c/c_m$) profiles of scalar fluctuations are shown in figure 5. Here, C and c are respectively the mean and r.m.s of concentration while C_m

and c_m are respectively their maxima. [1] suggested that a reflected Gaussian model, shown in eq. 1, closely describes the mean and r.m.s profiles of concentrations fluctuations for an elevated source. We note that our experimental data agree very well with the empirical model,

$$C(z) = C_0(s_z)\{\exp(-a(z+s_z)^2/\delta_z^2) + \exp(-a(z-s_z)^2/\delta_z^2)\}. \tag{1}$$

Here, a is taken to be $\ln(2)$ so that δ_z represents the vertical half-plume width (the vertical distance in which the maximum concentration falls to half its value). Although both mean and r.m.s profiles have reflected Gaussian behaviour, the plume width, δ_z, derived from them is different. The r.m.s profile has a greater spread than the mean concentration profile. Also, one can see that C_0 in the Gaussian model is dependent on s_z and C_m. Substituting $z = s_z$ in the above equation, we get, $C_m = C_0\{\exp(-a(4s_z^2/\delta_z^2))\}$. Based on the Gaussian model, it is easy to see that the plume spreads in both the vertical and lateral directions downstream of the source location.

Probability density functions

Another aspect of concentration measurements is the behaviour of probability density functions (PDF), which describe the likelihood of certain concentration level of tracer gas to occur at a point in space. Figure 6 shows the PDFs at several wall-normal locations for $s_z/\delta = 0.1$. It is evident that at most locations, the PDFs exhibit exponential-like behaviour ($\mathcal{P}(\tilde{C}) \sim \exp(-b\tilde{C})$, where b is the decay exponent) as seen from their linear behaviour with $\tilde{C} > C_m$ in the log-linear axes used in figure 6, however with different slopes. Interestingly, we observed that the PDFs at z locations that lie within the log-region have the same slope and this is being further investigated to develop a model for PDFs at high instantaneous concentration.

Conclusion

Both velocity and concentration measurements are carried out in a turbulent boundary layer with mild streamwise favourable pressure gradient. A well-established photo-ionisation technique is employed to measure concentration. The small size of PID needle enabled us to obtain concentration measurements with good spatial resolution. The effect of discharge tube on mean statistics of turbulent boundary layer is seen only when PID is in close proximity to the wall. The distributions of mean and variance of concentration fluctuations showed reflected Gaussian behaviour with different plume-widths in agreement with previously reported results. Further, the PDFs at most z locations exhibit exponential behaviour with identical decay exponents in the log-region of the boundary layer. As stated before, the future scope of this work is to conduct a series of experiments by varying s_x and s_z to investigate several aspects of plume dispersion, such as eddy-diffusivity and its relationship to eddy viscosity, the behaviour of PDFs in the log- and the intermittent region of TBL among others.

References

[1] Fackrell, J. E. and Robins, A. G., Concentration fluctuations and fluxes in plumes from point sources in a turbulent boundary layer, *J. Fluid Mech*, **117**, 1982, 26.

[2] Gifford, F., Statistical properties of a fluctuating plume dispersion model, *Adv. Geophys.*, **6**, 1959, 117–137.

[3] Harun, Z., Monty, J. P., Mathis, R. and Marusic, I., Pressure gradient effects on the large-scale structure of turbulent boundary layers, *J. Fluid Mech.*, **715**, 2013, 477–498.
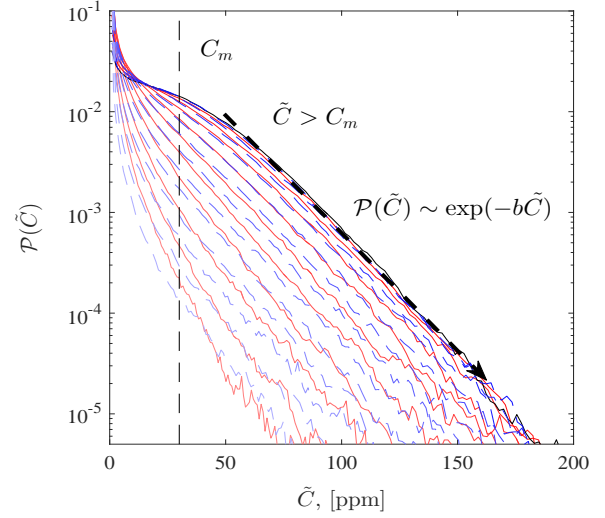
Figure 6: Probability density distributions at different wall-normal locations for $s_z/\delta = 0.1$. The blue dashed lines represent the PDFs at $z \le s_z$ and the red lines represent those above the source height, $z > s_z$. The vertical black dashed line shows the maxima in mean concentration, C_m. The exponential behaviour of PDF is shown as the black dashed line for $\tilde{C} > C_m$.

[4] Hay, J. S. and Pasquill, F., Diffusion from a continuous source in relation to the spectrum and scale of turbulence, *Adv. Geophys.*, **6**, 1959, 345–365.

[5] Ligrani, P. M. and Bradshaw, P., Spatial resolution and measurement of turbulence in the viscous sublayer using subminiature hot-wire probes, *Exp. Fluids*, **5**, 1987, 407–417.

[6] Marusic, I., Chauhan, K. A., Kulandaivelu, V. and Hutchins, N., Evolution of zero-pressure-gradient boundary layers from different tripping conditions, *J. Fluid Mech.*, **783**, 2015, 379–411.

[7] Marusic, I., McKeon, B. J., Monkewitz, P. A., Nagib, H. M., Smits, A. J. and Sreenivasan, K. R., Wall-bounded turbulent flows at high Reynolds numbers: Recent advances and key issues, *Phys. Fluids*, **22**, 2010, 065103.

[8] Metzger, M. M. and Klewicki, J. C., Development and characterization of a probe to measure scalar transport, *Meas. Sci. Tech.*, **14**, 2003, 1437.

[9] Nironi, C., Salizzoni, P., Marro, M., Mejean, P., Grosjean, N. and Soulhac, L., Dispersion of a passive scalar fluctuating plume in a turbulent boundary layer. Part I: Velocity and concentration measurements, *Boundary-Layer Meteorology*, **156**, 2015, 415–446.

[10] Smits, A. J., McKeon, B. J. and Marusic, I., High-reynolds number wall turbulence, *Annu. Rev. Fluid Mech.*, **43**, 2011, 353–375.

[11] Talluru, K. M., Kulandaivelu, V., Hutchins, N. and Marusic, I., A calibration technique to correct sensor drift issues in hot-wire anemometry, *Meas. Sci. Tech.*, **25**, 2014, 105304.

[12] Yee, E., Kosteniuk, P., Chandler, G., Biltoft, C. and Bowers, J., Statistical characteristics of concentration fluctuations in dispersing plumes in the atmospheric surface layer, *Boundary-Layer Meteorology*, **65**, 1993, 69–109.